03,08

On the possibilities of ab initio modeling for electron-phonon relaxation and transport properties by the examples of cadmium oxide and strontium titanate

© V.P. Zhukov[1], E.V. Chulkov[2,3]

[1] Institute of Solid State Chemistry, Russian Academy of Sciences, Ural Branch, Yekaterinburg, Russia
[2] St. Petersburg State University, St. Petersburg, Russia
[3] Dpto. de Polímeros y Materiales Avanzados: Física, Química y Tecnología, Facultad de Ciencias Químicas, Aptdo. 1072, 20018, San Sebastián, España

E-mail: Zhukov@ihim.uran.ru

Received December 2, 2021
Revised December 20, 2021
Accepted December 20, 2021

The calculations of the electron-phonon relaxation time, Seebeck coefficient and conductivity were performed for cadmium oxide with oxygen vacancies and strontium titanate doped with niobium using the first-principle methods based on the electron density functional perturbation theory, Boltzmann theory and many-body theory of electron-phonon interaction. It is shown that the calculations of relaxation time based on the many-body theory lead to significantly more accurate results on transport characteristics than in the case of the standard approximation of a constant relaxation time. It is shown that interaction with defects has a significant effect on conductivity.

Keywords: cadmium oxide, strontium titanate, electronic structure, PAW method, Boltzmann theory, transport characteristics.

DOI: 10.21883/PSS.2022.04.53496.249

1. Introduction

The last decade was marked by considerable success in development of methods for „ab initio“ modeling of solid state thermoelectric properties. The Boltzmann theories, electron density functional theory and many-body theory of the condensed state were used to develop a mathematical technique for calculation of electron-phonon (EP) interaction [1,2], electron conductivity, mobility, Hall and Seebeck coefficients, thermal conductivity [3–5], characteristics of superconductivity and dynamics of electron-phonon relaxation [6]. The developed approaches were used to implement programs for calculating of the specified solid state characteristics on the basis of the previously developed software packages of electronic band structure calculation [7–11]. Many calculations of the given characteristics were performed for metals and undoped semiconductors, which reasonably agreed with the experimental data (see the reviews [12–17]).

However, the prospects of use of the developed approaches in calculating the properties of doped semiconductors or alloys remain vague. Only a few papers were dedicated to calculations of semiconductors having different doping element concentrations [18,19]. They used an approach based on the Boltzmann theory with a fixed time of electron-phonon (EP) relaxation [3,4] without comparison with experimental data. Approximation of a fixed time of EP-relaxation considerably reduces the necessary computer resources for calculations, therefore, its use is a standard technique. However, the studies performed for doped semiconductors do not allow for estimating the accuracy of obtained results, so that additional effort are required in this area.

Since both CdO and $SrTiO_3$ are widely used in many areas of modern engineering, these compounds attract considerable attention of researchers, therefore many investigations to study their properties have been carried out. These compounds in the initial state are semiconductors with the band gap of 0.8 eV for CdO and 3.25 eV for $SrTiO_3$, however, they can be changed over to the state of *n*-conductors by introduction of vacancies into the oxygen sublattice or by heterovalent doping. Experimental studies of CdO transport characteristics were performed in [20–22], and similar studies for $SrTiO_3$ — in [23–25]. In [20–22], conductivity in CdO was achieved due to the formation of oxygen vacancies during high-temperature annealing, while for $SrTiO_3$ in [23–25] it was achieved due to doping with Ta, Pr or Nb. Dependences of the Seebeck coefficient, conductivity, thermal conductivity, carrier concentration and carrier mobility on annealing temperature and doping were obtained. These papers contain sufficient data for checking correctness of the „ab initio“ methods for transport properties calculation, which is the main goal of our calculations.

In this paper we present the calculations of the Seebeck coefficient and conductivity performed within the frame-

work of two approaches implemented in the BoltzTraP-1 software package [3], and in the newest PERTURBO package [6]. These calculations make it possible to estimate accuracy of calculations of transport characteristics, to reveal disadvantages and advantages of the approaches and presence of problems to be solved.

2. Theoretical framework

Ab initio methods for calculation of solid state transport characteristics are based on a combination of the Boltzmann phenomenological theory of transport and methods for calculating of current carrier scattering resulting from the many-body theory of the solid state. The present day state of the Boltzmann theory is detailed in literature [5,26–28]. The fundamentals of the methods for calculation of current carrier scattering on phonons are outlined in [1,2]. Computer codes for calculation of transport properties use the previously developed methods for calculating the electronic band structure based on the electron density functional theory (DFT) [29] and phonons based on the DFT perturbation theory [1]. The code construction principles are described in [3,4,6,10], therefore we will only dwell upon some aspects of the theory important for discussion of the obtained results.

According to the first Onsager equation [30], current density in condensed medium j is related to electric field intensity E and temperature gradient ∇T, generated by external sources, by the relation

$$j = \sigma E - K\nabla T. \tag{1}$$

It is supposed that intensity and gradient in a solid can be non-collinear to current, i.e. σ and K are tensor quantities. The Seebeck coefficient for a homogeneous medium is conventionally determined as a coefficient of proportionality between electric field intensity and temperature gradient, i.e. $E = S\nabla T$, provided that current is absent. Then a generalization of the Seebeck coefficient, according to (1), will be a tensor quantity

$$S = \sigma^{-1}K. \tag{2}$$

A relation between σ, K, S and material's electronic structure is established on the basis of the Boltzmann theory. The main assumption in this theory is that the electron distribution function in a material $f(r,k,t)$ at a small intensity and a small temperature gradient differs little from the standard Fermi function.

$$f_0(r,k) = \frac{1}{e^{[\varepsilon(k)-\mu]/k_B T(r)}+1}. \tag{3}$$

Here only temperature depends on the coordinate, while the fixed chemical potential depends only on material properties. Another assumption of the theory is the so-called relaxation time approximation (RTA), which considers that if external fields are activated at time moment $t = 0$, then the deviation of the distribution function from the stationary one upon their withdrawal at time moment t changes according to

$$f(r,k,t) = \left[f(r,k,0) - f_0(r,k)\right]e^{-t/\tau(k)}, \tag{4}$$

i.e. the distribution function returns to the initial state at a rate determined by characteristic relaxation time $\tau(k)$. The solution of the Boltzmann equation in this approximation assumes the form, see [28],

$$f(r,k) = f_0(r,k) - \frac{\partial f_0}{\partial \varepsilon}\tau(k)v(k)\left[-eE + \frac{\varepsilon(k)-\mu}{T}\nabla T\right], \tag{5}$$

where $v(k)$ is electron group velocity in state $\varepsilon(k)$.

Current carried by electrons, taking into account the fact that the stationary distribution function makes no contribution and neglecting the contribution from temperature gradient, can be calculated as

$$j = \frac{e}{4\pi^3}\int d^3k v\, f(r,k) = -\frac{e^2}{4\pi^3}\int d^3k\,\tau(k)\left(-\frac{\partial f_0}{\partial \varepsilon}\right)[v\otimes v]E. \tag{6}$$

That is, the tensor of electrical conductivity is written as [5]:

$$\sigma = -\frac{e^2}{4\pi^3}\int d^3k\tau(k)\left(-\frac{\partial f_0}{\partial \varepsilon}\right)[v\otimes v]E. \tag{7}$$

Considering the contribution to the distribution function from the temperature gradient, total current can be presented as

$$j = \sigma E + \frac{1}{4\pi^3}\int d^3k v\left(-\frac{\partial f_0}{\partial \varepsilon}\right)\tau(k)\frac{\varepsilon-\mu}{T}(v\nabla T). \tag{8}$$

It follows that if a tensor is introduced,

$$L^{(n)} = \frac{1}{4\pi^3}\int d^3k\left(-\frac{\partial f_0}{\partial \varepsilon}\right)\tau(k)(\varepsilon-\mu)^n[v\otimes v], \tag{9}$$

as usually done in the transport theory, the tensor expressions assume the form

$$\sigma = L^{(0)}, \tag{10}$$

$$S = [L^{(0)}]^{-1}L^{(1)}\frac{1}{T}, \tag{11}$$

$$K = L^{(1)}\frac{1}{T}. \tag{12}$$

If we assume that relaxation time does not depend on energy and the wave vector, the Seebeck tensor becomes time-independent. This assumption is the ground of the codes [3,4], and the result is a drastic increase of their speed of operation. However, we well show later that this approximation makes the calculations considerably less accurate, leastways for the compounds under consideration.

Thereat, the dependence σ on τ is maintained, therefore the results in literature are usually reported as σ/τ.

„Ab initio“ calculations of electron-phonon contribution to relaxation time based on the Migdal–Eliashberg theory [31,32] have been implemented recently in codes [10,16]. This theory suggests that electron relaxation in state $|\psi_{n,\mathbf{k}}\rangle$, where n-number of band structure branch, occurs due to transitions to states $|\psi_{m,\mathbf{k}+\mathbf{q}}\rangle$ because of absorption or emission of phonons with wave vectors $\mathbf{q}$ and energy $\omega_{\mathbf{q}\nu} = \varepsilon_{m,\mathbf{k}+\mathbf{q}} - \varepsilon_{n,\mathbf{k}}$. Transition probabilities in the first order of the perturbation theory are determined by matrix elements

$$g_{mn,\nu}(\mathbf{k}, \mathbf{q}) = \langle \psi_{m,\mathbf{k}+\mathbf{q}} | \partial_{\mathbf{q}\nu} V | \psi_{n,\mathbf{k}} \rangle, \qquad (13)$$

where $\partial_{\mathbf{q}\nu} V$ is the derivative of the self-consistent potential with respect to phonon perturbation with wave vector $\mathbf{q}$ and polarization index ν. The methods for calculation of matrix elements based on the DFT perturbation theory in the plane wave basis are described in [33], and in the basis of localized Wannier functions — in [1,6,10].

Contemporary implementations of the electron-phonon interaction theory are based on the formalism of the self-energy operator of the many-body solid state theory. In this approach, the change of electronic state energy due to electron-phonon interaction and state width are respectively determined, within the framework of RTA approximation [6,11], by the real and imaginary parts of the self-energy $\Sigma_{n\mathbf{k}} = \Sigma'_{n\mathbf{k}} + i\Sigma''_{n\mathbf{k}}$, which can be calculated as [11]:

$$\sum n\mathbf{k} = \sum_{\mathbf{q}\nu} w_{\mathbf{q}} |\mathbf{g}_{mn,\nu}(\mathbf{k}, \mathbf{q})|^2 \left[\frac{\mathbf{n}(\omega_{\mathbf{q}\nu}) + \mathbf{f}_0(\varepsilon_{m,\mathbf{k}+\mathbf{q}})}{\varepsilon_{n,\mathbf{k}} - \varepsilon_{m,\mathbf{k}+\mathbf{q}} - \omega_{\mathbf{q}\nu} - \mathbf{i}\eta} \right.$$

$$\left. + \frac{\mathbf{n}(\omega_{\mathbf{q}\nu}) + 1 - \mathbf{f}_0(\varepsilon_{m,\mathbf{k}+\mathbf{q}})}{\varepsilon_{\mathbf{n},\mathbf{k}} - \varepsilon_{m,\mathbf{k}+\mathbf{q}} + \omega_{\mathbf{q}\nu} - \mathbf{i}\eta} \right], \qquad (14)$$

where $n(\omega_{\mathbf{q}\nu})$ is the Bose–Einstein distribution function. Then, according to the „time–energy“ uncertainty principle, time of electron state relaxation due to interaction with phonons can be calculated as

$$\tau_{n\mathbf{k}}(T) = \frac{1}{2\Sigma''_{n\mathbf{k}}(T)}. \qquad (15)$$

Calculations $\tau_{n\mathbf{k}}$ were implemented in codes [5,6,10]. The main problem of such calculations is their demand for considerably greater computer resources than calculations with fixed τ, which is first of all associated with the need to calculate phonon states with a set of wave vectors distribution in the irreducible part of the Brillouin zone. Therefore, calculations of transport properties in this approach are possible for systems which are relatively simple as compared to systems available in calculations with fixed τ. However, it will be shown below that the calculations of relaxation time, leastways for the compounds under consideration, yield considerably more accurate results.

Calculated and experimental values of phonon frequencies for the Γ-point of the Brillouin zone in $SrTiO_3$ and CdO

$SrTiO_3$		
This paper (cm^{-1})	Previously calculated [40,41] (cm^{-1})	Experimental — see [40,41] (cm^{-1})
66	50	42, 91
165	160, 170	170, 175
518	562	545, 547
CdO		
265	267	265
485	431	523

3. Calculation details

The electronic band structure was calculated for the FCC-structure of CdO and the simple cubic structure of $SrTiO_3$ by the pseudo-potential method in the plane wave basis implemented in the Quantum Espresso software package [8]. The calculations were initially performed for 16 wave vectors in the irreducible part of the Brillouin zone in the case of CdO and for 10 vectors for $SrTiO_3$. In both cases, plane waves with energy up to 80 Ry were used in the band state representation, and up to 600 Ry in the electron density representation. It is known that phonon calculations using the DFT perturbation theory are sensitive to the kind of used pseudopotentials (PP), in particular, for low-energy phonons. Therefore, we have tried 7 PP types. Calculations were performed using PAW pseudopotentials according to Kresse–Joubert (KJPAW) [34] with the exchange-correlation part according to Perdew–Burke–Ernzerhof (PBE) [35] and a similar PP for a solid body (PBESOL) [36]. We also used ultra-soft PPs according to Rappe–Rabe–Kaxiras–Joannopoulos (RRKJUS) [37] with an exchange-correlation part of the PBE, PBESOL type [29,30], as well as PPs according to Vanderbilt (VAN) [38] with Perdew–Wang exchange-correlation (PW) [39]. Phonon states were calculated on the basis of electron state calculations by the method of the DFT perturbation theory [8]. The best results, partially given in the table, for CdO were provided by calculations with PAW PPs by the PBE–KJPAW method, and for $SrTiO_3$ — with ultra-soft PPs using the PW–PBE method. A comparison with the results of the previous calculations by similar methods (Quantum Espresso [40] and Abinit codes [41]) show a calculation accuracy typical for DFT perturbation theory methods.

However, like most DFT-based calculations of electronic band states, our calculations give underestimated band gap values: for $SrTiO_3$ it is equal to 1.84 eV, while for CdO the states near the top of valence band the conduction band states. It will be further shown that this error for $SrTiO_3$,

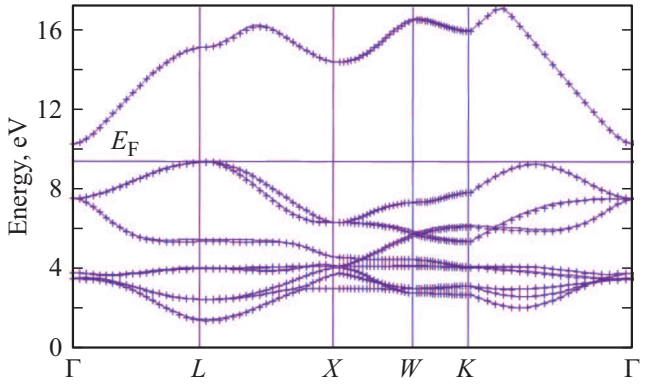

Figure 1. Dispersion curves for the principal directions in the cadmium oxide Brillouin zone. The crosses mark the calculation results in the plane wave basis (the Quantum Espresso software). The solid lines corresponds to the band states calculated in the basis of Wannier functions using the procedure [46].

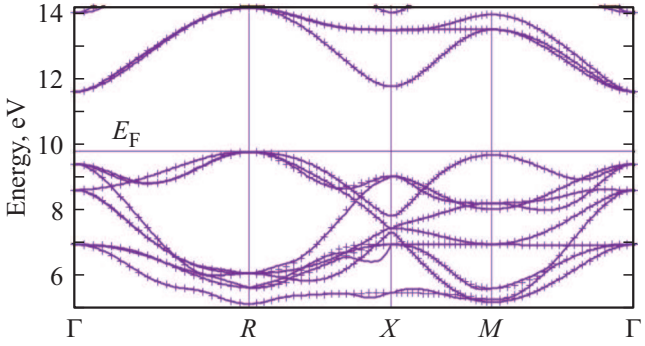

Figure 2. Dispersion curves for the band states of strontium titanate. The solid lines corresponds to the calculation results in the Wannier basis [40], while the crosses mark the band states obtained in the plane wave basis.

i.e. when the band gap is present in calculations, apparently, does not give rise to complications in calculations of transport characteristics. However, an overlap of the valence band with the conduction band yields incorrect results for cadmium oxide: contrary to the experiment, the Seebeck coefficient turns out to be positive at all considered current carrier concentrations. In order to eliminate this error, the CdO band states were recalculated by introducing a single-center Hubbard correction with the parameter U by the method described in [42] to exchange-correlation potential for $2p$-orbitals of the oxygen atom. With $U = 6$ eV the band gap, 0.91 eV, agrees well with the experimental data; at the same time, this correction eliminates the problem in Seebeck coefficient calculations. According to the previous experimental and calculated data [35,43–45], the band gap is indirect, between the L and Γ points for CdO and $R-\Gamma$ for $SrTiO_3$. The dispersion curves of electronic states for CdO and $SrTiO_3$, obtained in the plane wave basis, are shown in Fig. 1 and 2. The Fermi level is near the conduction band bottom at all the experimentally studied current carrier concentrations [22–25], from $\sim 1 \cdot 10^{19}$ to $\sim 15 \cdot 10^{19}$ 1/cm^3. The conduction band states in case of CdO are formed by $5s$ Cd-orbitals, and in case of $SrTiO_3$ — by $3d$ Ti-orbitals. The Fermi level for CdO is intersected by one branch of band states, and for $SrTiO_3$ — by one branch of states near the point X and three branches near the point Γ.

The calculations of electron and phonon states were used to calculate the transport characteristics in CdO and $SrTiO_3$ by the methods described in [3], the BoltzTaP-1 program, and in [6], the Perturbo program. The problem of transport properties calculation, as has already been mentioned many times [3,4,10], is their demand for calculation of a large number of band states near the Fermi level, for a number of wave vectors 100 000 minimum per the full Brillouin zone. This problem is solved in method [3] by a Fourier interpolation between the states obtained in the plane wave basis.

A similar problem, in the later methods [6,10,11], is solved by a transition from the Bloch function basis to the basis of localized Wannier functions by the methods described in [46]. The Wannier basis can be used to obtain a set of band states for a very large number of wave vectors in the Brillouin zone. Evidently, states obtained in the Wannier basis must correspond well to their equivalents obtained in the plane wave basis. A significant role is played by selection of the starting localized states which in the iteration processes described in [46] are converted into a Wannier basis. The starting states for CdO in our case were $5s$-, $5p$-states of cadmium atoms and $2s$-, $2p$-states of oxygen atoms. The $3d$ Ti- and $2p$ O-states were used as a starting basis for $SrTiO_3$. It follows from Fig. 1 that the CdO state energies in the Wannier basis are almost the same as the energies in the plane wave basis. Quality of band states obtained in the Wannier basis for $SrTiO_3$ is characterized in Fig. 2. It follows that the state energies, obtained in the Wannier basis, in the valence band upper part from 7.5 to 10 eV, and in the conduction band part from 11.5 to 14 eV, are virtually the same as the energies of their equivalents in the plane wave basis. There are several differences for the wave vectors near the point X in the range of 5 to 7 eV, however, they are insignificant in calculations of transport properties. This confirms the correct choice of the Wannier basis. Therefore, the calculations of transport properties both for CdO and for $SrTiO_3$ were performed using band states in the Wannier basis, obtained for 125 000 wave vectors in a full Brillouin zone. Since the available experimental data shows an electronic nature of conduction, we took into account only the band states in the interval of ± 0.5 eV from the Fermi level, which corresponds to the experimentally obtained carrier concentration values. The corresponding state densities near the conduction band bottom are shown in Fig. 3.

The peculiarity of calculations using the method [6] is that probabilities of electron transitions between states with wave vectors $\mathbf{k}$ and $\mathbf{k}+\mathbf{q}$, generated due to involvement of phonons with wave vectors $\mathbf{q}$, are calculated for a large

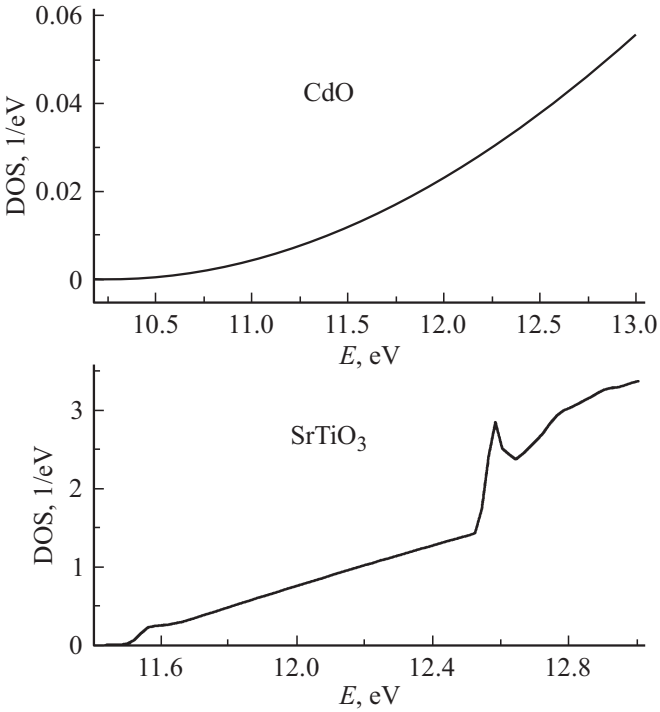

Figure 3. The densities of states near the conduction band bottom for CdO and $SrTiO_3$.

set of randomly chosen vectors **q**. The set of **q** in our calculations, as recommended by the program authors [6], included 1 000 000 vectors.

4. Results and discussion

In this section we compare the calculated transport characteristics with the experimental data of [22] for CdO and [25] for $SrTiO_3$, where dependences of transport properties on carrier concentration are presented most fully. In [22], carrier concentrations at the annealing temperatures of 700, 800, 900 and 1000 K were $(0.75, 2.51, 3.75, 4.28) \cdot 10^{19}$ 1/cm^3 respectively. The concentration of niobium impurities in $SrTiO_3$ was from 2 to 6%, which corresponds to the carrier concentration of $(4.79, 5.98, 7.98, 9.57, 10.30) \cdot 10^{19}$ 1/cm^3. The transport characteristics were calculated for these concentrations.

Fig. 4 for CdO, along with the corresponding experimental data, gives the temperature and concentration dependences of Seebeck coefficient S calculated using the procedures [3] (BoltzTraP-1 code) and [6] (Perturbo). (Due to the cubic symmetry, $S = S_{xx} = S_{yy} = S_{zz}$, while nondiagonal elements of the Seebeck tensor are negligible). It can be seen that the results obtained using the BoltzTraP-1 procedure correctly reflect only the temperature dependence of S. As distinct from the experiment results, their values at 300 K are virtually independent from carrier concentration and in magnitude are, on the average, underestimated. The results obtained using the Perturbo procedure, both in terms of the magnitude of Seebeck coefficient and in terms of temperature dependence, up to 900 K, agree well with the experimental data, particularly for high carrier concentrations. They also agree with the experimentally observed decrease of the magnitude of S when the carrier concentration increases.

Fig. 5 shows the concentration and temperature dependences of CdO resistivity using two procedures. Resistance calculations according to Boltztrap-1 [3] require an independent estimation of relaxation time. We performed such an estimation by fitting the values of $(\sigma/\tau)_{\text{calc}}$, calculated for $T = 300$ K and the aforesaid carrier concentrations, to the available experimental values of resistivity ρ_{exp} at the specified concentrations, which corresponds to formula $\tau = \frac{1}{\rho_{\text{exp}}(\sigma/\tau)_{\text{calc}}}$. Averaging by carrier concentration values yields a value of τ for cadmium oxide equal to 7.6 fs. As compared to experiment, the calculated resisitivity at a temperature of about 300 K are underestimated according to both procedures, while resistance increase with temperature according to the Perturbo procedure is overestimated, and almost absent according to Boltztrap-1. The absence of resistivity increase according to BoltzTraP-1 cannot be justified in any way. However, the underestimated

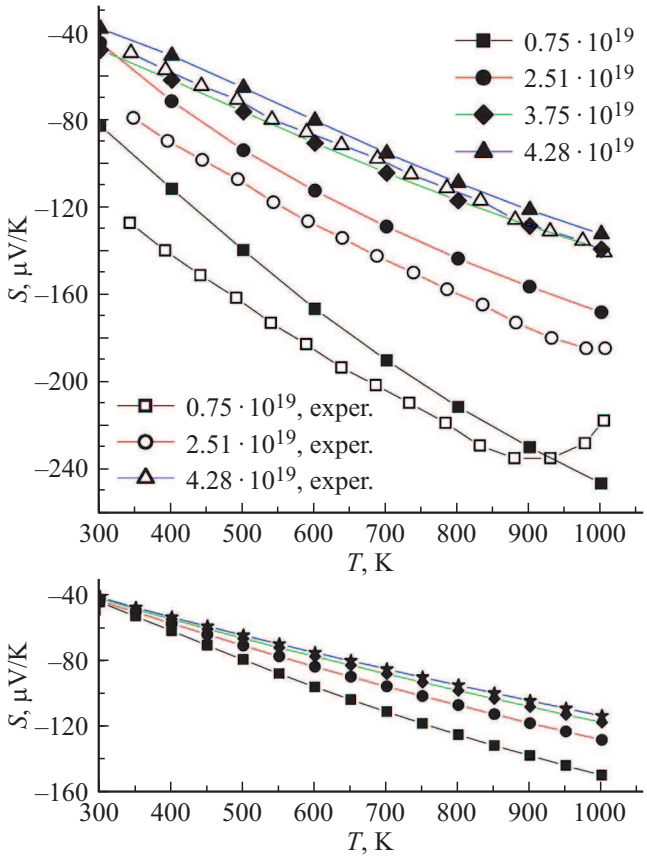

Figure 4. Concentration and temperature dependences of Seebeck coefficient for cadmium oxide. The calculated data in the upper panel were obtained using the procedure [6], and on the lower one — using the procedure [3]. The experimental data was taken from [22].

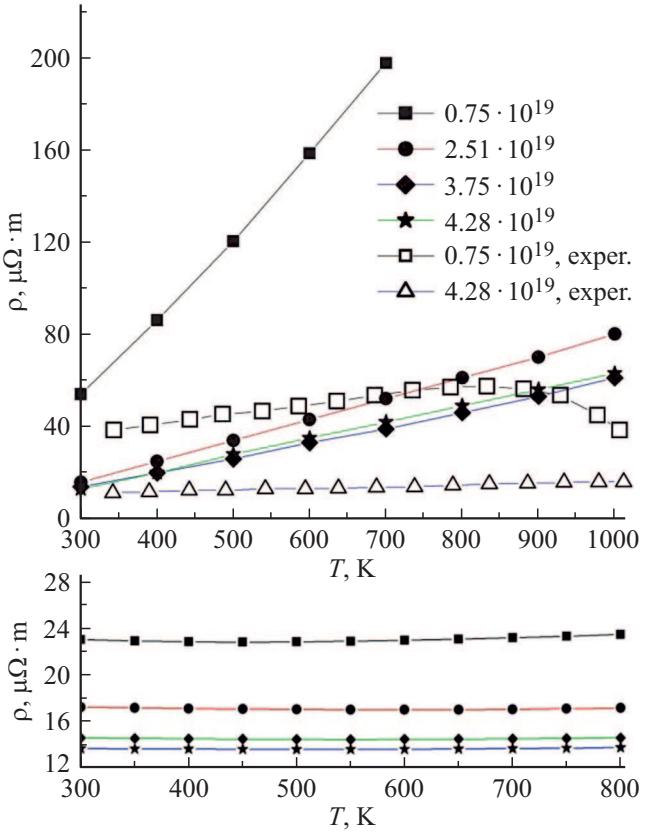

Figure 5. Concentration and temperature dependences of cadmium oxide resistivity. The calculated data in the upper panel were obtained using the Perturbo procedure [6], and on the lower one using the Boltztrap-1 procedure [3]. The experimental data is from [22].

resisitivity at 300 K and its excessively high temperature coefficient in the Perturbo procedure are explained by the fact that a considerable contribution to resisitivity is, possibly, provided by defect scattering, in this case probably on oxygen vacancies with charge +2. It is known that this scattering is proportional to defect concentration, but does not depend on temperature [28]. According to the Matthiessen's rule [26]:

$$\frac{1}{\tau} = \frac{1}{\tau_{e-ph}} + \frac{1}{\tau_{e-def}} \qquad (16)$$

when adding the rate of electron-phonon relaxation, determined by time τ_{e-ph}, to the rate of electron-defect relaxation dependent on τ_{e-def}, temperature coefficient of total relaxation time τ, i.e. resistance as well, must decrease. It can be also seen that the temperature coefficient of resistance decreases with vacancy concentration increase, which agrees with the intensification of scattering by vacancies. We will demonstrate below that the conclusion on an important role of interaction with defects also agrees with the results for $SrTiO_3$.

Fig. 6 shows the calculated and experimental data [25] for the Seebeck coefficient of $SrTiO_3$.

It can be seen that the results obtained using the Boltzmann-1 procedure reproduce well the temperature dependence of the Seebeck coefficient, but are overestimated by more than 50 μV/K and do not reflect the dependence of S on carrier concentration. On the contrary, the results obtained according to the Perturbo procedure, up to $\sim$ 500 K almost perfectly agree with the experimental dependences on concentration and temperature. The experimental data at $T > 500$ K deviates from the regularities, represented by the experimental data at lower temperatures, which, apparently, indicates changes of the crystalline structure parameters at high temperatures. This assumption is justified in the results of [47] where it was shown that a threefold reduction of crystallite sizes and a 0.3% reduction of the lattice spacing are observed (when temperature increases from 500 to 600 K) in the $SrTiO_3$ samples, obtained by electron-beam evaporation and microwave sputtering.

Fig. 7 shows the theoretical and experimental values of $SrTiO_3$ resistivity. Relaxation time in calculations using the Boltztrap-1 procedure was estimated using the same procedure as for cadmium oxide; it was equal to 3.2 fs. The results obtained using this procedure demonstrate, contrary to the experiment, a very weak dependence of resistivity — both on carrier concentration and on temperature. As regards the Perturbo procedure, the obtained results at 300 K with all carrier concentrations, except the maximum one, agree well with the experimental data. As in the case of CdO, the temperature dependence of resistivity is overestimated, but the overestimation degree is significantly smaller. Similarly to cadmium oxide, we can assume that

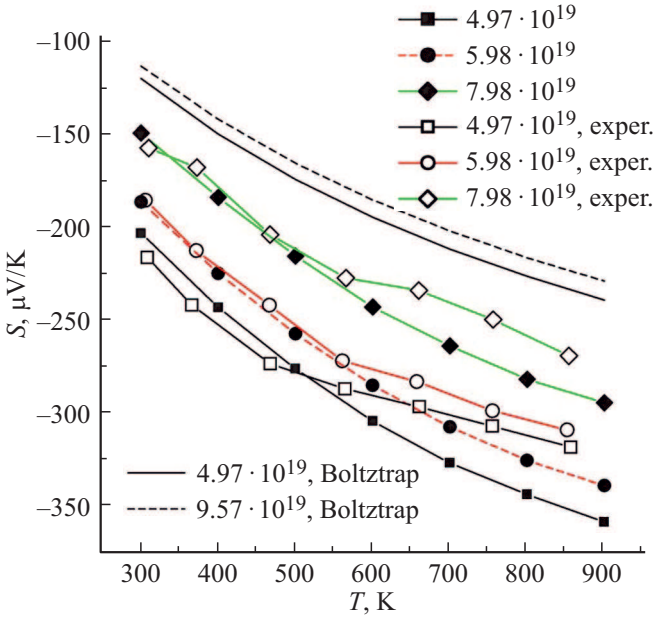

Figure 6. Concentration and temperature dependences of Seebeck coefficient for $SrTiO_3$. The calculated data were obtained using the Perturbo procedure [6] and using the Boltzman-1 procedure [3]. The experimental data was taken from [25].

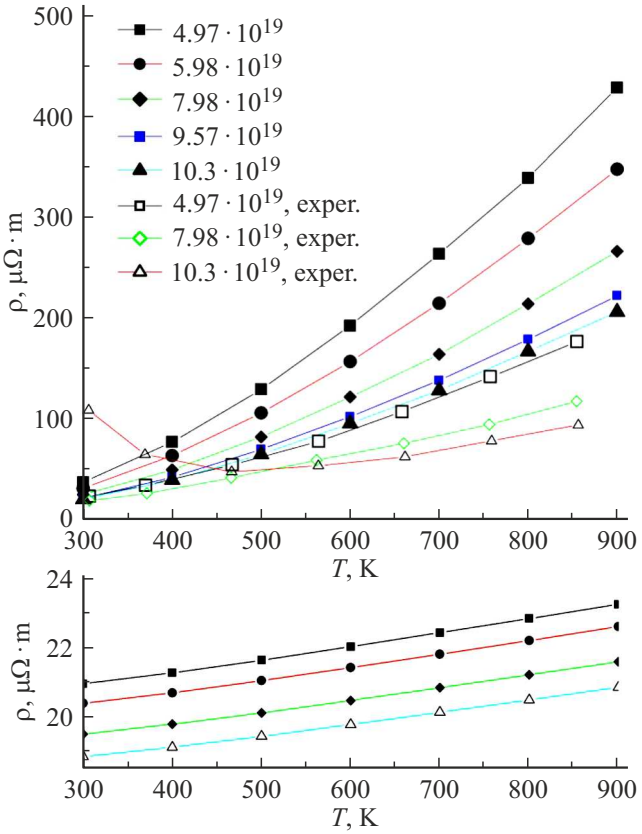

Figure 7. Concentration and temperature dependences of $SrTiO_3$ resistivity. The calculated data in the upper panel were obtained using the Perturbo procedure [6], and on the lower one — using the Boltzman-1 procedure [3]. Experimental data — see [25].

this mismatch is due to the fact that our calculations do not take into account defect scattering of carriers. According to [28], defect scattering rate is proportional to the square of their effective charge. It follows that niobium impurity scattering is approximately 4 times weaker than oxygen vacancy scattering. This circumstance quite agrees with the smaller deviation of the temperature dependence of resistivity, calculated for $SrTiO_3$, from the experiment than in the case of CdO. When niobium impurity concentration increases, the calculated temperature dependence decreases and approaches the experimental one, which, like with CdO, can also be explained by an intensification of impurity scattering, independent from temperature.

On the whole, the resistivity calculations using the Perturbo procedure [6] provide higher-quality results than those using the Boltzman-1 procedure [3]. The most significant error in the calculation results using the Boltzman-1 procedure is the almost complete absence of resistivity dependence on temperature and defect concentration. Since the main difference of procedure [3] from procedure [6] is in the use (in the first case) of an approximation of a fixed relaxation time, this casts doubt on efficiency of use of such an approximation. Fig. 8 gives the data on the time of electron-phonon relaxation in CdO and $SrTiO_3$, calculated for electron states near the conduction band bottom at 300 K.

Depending on carrier concentration and temperature, the Fermi level shifts in the range of 10.15−10.25 eV for cadmium oxide and 11.41−11.61 for $SrTiO_3$, i.e. in both cases it is in the range of an abrupt relaxation time change. The average relaxation time can be considered constant only at an energy above ∼ 10.5 eV for CdO and above ∼ 11.7 for $SrTiO_3$, however, this can occur with a significantly higher carrier concentration than the one achievable in experiments. The disregard of the dependence of relaxation time on Fermi energy in the BoltzTrap-1 procedure causes the absence of resistance dependence on carrier concentration.

Since electron velocity in equations (6)−(9) does not depend on temperature, the experimentally observed resistance increase with temperature rise is in most cases, probably, associated with relaxation time decrease. Fig. 9 shows the dependences on temperature and carrier concentration for the relaxation time of CdO and $SrTiO_3$ electron states, whose energy is the closest to the Fermi level, calculated using the Perturbo procedure. All the concentrations are characterized by relaxation time decrease with temperature, which correlates with temperature-dependent rise of resistance. However, relaxation time decreases at any

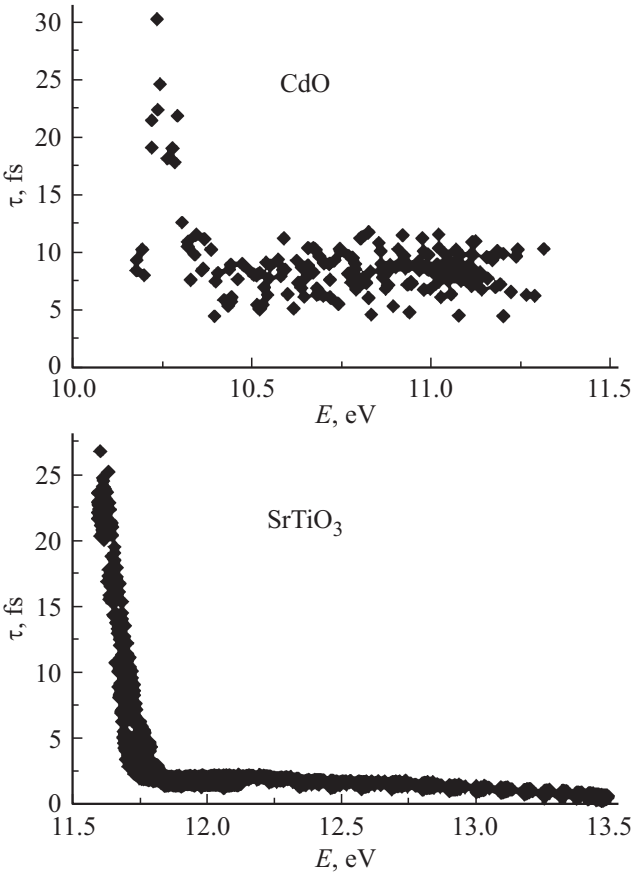

Figure 8. Calculated values of electron-phonon relaxation time for CdO and $SrTiO_3$ depending on electron state energy.

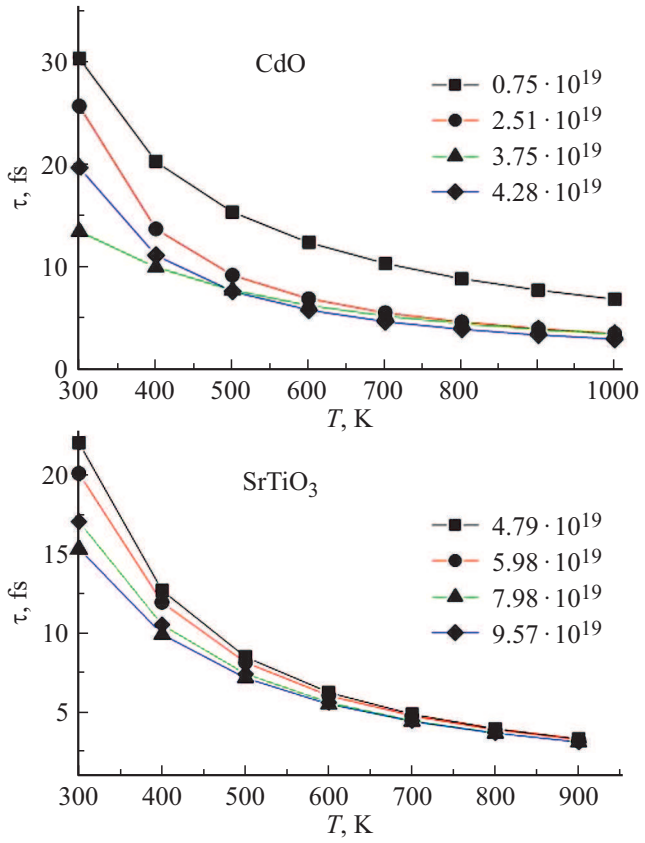

Figure 9. Temperature dependences of relaxation time for electron state with energies, maximum close to the Fermi level, calculated for CdO and $SrTiO_3$.

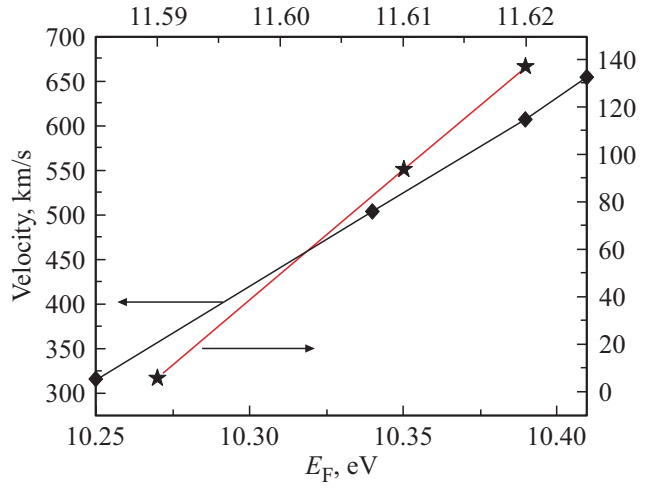

Figure 10. Dependences of average electron velocity at the Fermi level on Fermi energy.

fixed temperature with an increase in carrier concentration, which contradicts the resistivity decrease at this temperature. One of the factors that increase conductivity at an increase in carrier concentration, i.e. that reduce resistivity, is an increase of state density at the Fermi level, evident in Fig. 3.

Another factor accountable for resistivity decrease is an increase of electron velocity at the Fermi level. According to Fig. 10, it occurs both for CdO and for $SrTiO_3$ for cadmium oxide (rhombi) and strontium titanate (stars).

5. Conclusion

By the example of cadmium oxide with oxygen vacancies and niobium-doped strontium titanate, we estimated the degree of correctness of the Seebeck coefficient and resistivity calculations using two „ab initio“ procedures, based on the Boltzmann theory and implemented in the Boltztrap-1 [3] and Perturbo software packages [6]. It follows from the calculations that the Boltztrap-1 procedure has a limited accuracy: the obtained Seebeck coefficient values are underestimated in absolute magnitude and do not reproduce the experimentally observed dependences on temperature and carrier concentration. More correct results are provided by calculations using the Perturbo procedure, which includes an „ab initio“ estimation of relaxation time. The performed calculations of electron-phonon relaxation time indicate that both CdO and $SrTiO_3$ are characterized by a considerable dependence of relaxation time on carrier concentration and temperature.

The ignoring of these dependences in the Boltztrap-1 procedure seems to be the main reason for evening-out of the dependence of the Seebeck coefficient and resistivity on carrier concentration and temperature. The Perturbo procedure for CdO in almost all cases agrees well with the experiment. The same procedure in the case of $SrTiO_3$ at temperatures up to 500 K leads to an almost perfect agreement of the calculated Seebeck coefficient with the experimental data. The success of the Seebeck coefficient calculation is probably due to the fact that, according to equation (11), the errors in relaxation time calculation during its computation are compensated due to division of tensors $L^{(1)}/L^{(0)}$. The observed deviations of the calculated data from the experimental data at temperatures above 500 K are probably due to the experimentally observed changes in the lattice spacing.

However, calculations using the Perturbo procedure lead to an overestimated dependence of resistivity on temperature. A comparison of the results for CdO and $SrTiO_3$ makes it possible to conclude that this shortcoming is due to the neglect of defect scattering of carriers, i.e. scattering by oxygen vacancies in CdO and Nb impurities in $SrTiO_3$. It should be noted that development of computer codes for „ab initio“ calculation of time of carrier relaxation on ionized defects is a topical problem not yet solved completely. Thus, the authors of the Perturbo procedure published a paper on vacancy scattering in silicon [48], but it was not followed by any developments. Another procedure that includes ionized impurity scattering was suggested in [49], but the procedure was not tested on doped semiconductors.

Attention is called to the anomalous change (non-reproducible in calculations) of the measured Seebeck coefficient and resistance of cadmium oxide with the carrier concentration of $0.75 \cdot 10^{19}$ 1/cm^3 at 800–1000 K, which means a transition to the semiconductor type of conduction at the said temperature. Semiconductor conductivity for doped $SrTiO_3$ is also observed at the maximum carrier concentration, $4.79 \cdot 10^{19}$ 1/cm^3 and a temperature from 300 to 500 K. A deviation of the calculation results from these anomalies is probably due to the fact that the calculations considered only the conduction band electrons which formed during vacancy origination or doping. Since the state density in valence band is high, the accounting of their contributions to conductivity requires incomparably more computer resources than the accounting of conduction band electrons only.

Funding

The work has been funded by the state budget. All calculations were performed at the URAN cluster of Mathematics and Mechanics Institute of the Ural Branch of RAS.

Conflict of interest

The authors declare that they have no conflict of interest.

References

[1] F. Giustino, M. L. Cohen, S.G. Louie. Phys. Rev. B **76**, 165108 (2007).
[2] F. Giustino. Rev. Mod. Phys. **89**, 015003 (2017).
[3] G.K.H. Madsen, D.J. Singh. Comp. Phys. Commun. **175**, 67 (2006).
[4] G.K.H. Madsen, J. Carrete, M.J. Verstraete. Comp. Phys. Commun. **231**, 140 (2018).
[5] T.J. Scheidemantel, C. Ambrosch-Draxl, T. Thonhauser, J.V. Badding, J.O. Sofo. Phys. Rev. B **68**, 125210 (2003).
[6] J.-J. Zhou, J. Park, I-T. Lu, I. Maliyov, X. Tong, M. Bernardi. Comp. Phys. Commun. **264**, 107970 (2021).
[7] G. Kresse, M. Marsman, J. Furthmüller. Vienna ab-initio simulation package. VASP the guide. UniversitätWien, Wien (2018). 233 p.
[8] P. Giannozzi, O. Andreussi, T. Brumme. J. Phys.: Condens. Matter. **29**, 465901 (2017).
[9] P. Blaha, K. Schwarz, F. Tran, R. Laskowski, G.K.H. Madsen, L.D. Marks. J. Chem. Phys. **152**, 074101 (2020).
[10] S. Ponce, E.R. Margine, C. Verdi, F. Giustino. arXiv:1604.03535
[11] J. Noffsinger, F. Giustino, B.D. Malone, Ch-H. Park, S.G. Louie, M.L. Cohen. Comp. Phys. Commun. **181**, 2140 (2010).
[12] A. Faghaninia. Theory of Carrier Transport From First Principles: Applications in Photovoltaic and Thermoelectric Materials. Dissertation. University of Washington (2016). 219 p.
[13] Y. Wang, Sh.-L. Shang, H. Fang, Z.-K. Liu, L.-Q. Chen. Comp. Mater. **2**, 16006 (2016).
[14] F. Ricci, W. Chen, U. Aydemir, G.J. Snyder, G.-M. Rignanese, A. Jain, G. Hautier. Scientific Data **4**, 17008 (2018).
[15] M. Yasukawa, K. Ueda, S. Fujitsu, H. Hosono. Ceram. Int. **43**, 9653 (2017).
[16] L. Lindsay, D.S. Parker. Phys. Rev. B **92**, 144301 (2015).
[17] A.A. Adewale, A. Chik, R.M. Zaki, F.Ch. Pa, Y.Ch. Keat, N.H. Jamil. Int. J. Nanoelectron. Mater. **12**, 477 (2019).
[18] M.U. Kahaly, U. Schwingenschlogl. J. Mater. Chem. A **2**, 10379 (2014).
[19] A. Mukasia, G.S. Manyali, H. Barasa, J. Sifuna. J. Mater. Sci. Res. Rev. **2**, 1 (2019).
[20] S.K. Vasheghani Farahani, V. Munoz-Sanjose, J. Zuniga-Perez, C.F. McConville, T.D. Veal. Appl. Phys. Lett. **102**, 022102 (2013).
[21] L. Qing, W.Sh. Fang, L.L. Jiang, W.J. Long, D.Sh. Yu, Y. Wei, F.G. Sheng. Sci. China-Phys. Mech. Astron **57**, 1644 (2014).
[22] X. Zhang, H. Li, J. Wang. J. Adv. Ceram. **4**, 226 (2015).
[23] Y. Cui, J.R. Salvador, J. Yang, H. Wang, G. Ampw, H. Klainke. J. Electron. Mater. **38**, 1002 (2009).
[24] A.V. Kovalevsky, A.A. Yaremchenko, S. Populoh, A. Weidenkaff, J.R. Frade. J. Appl. Phys. **113**, 053704 (2013).
[25] T.T. Khan, S.-Ch. Ur. Electron. Mater. Lett. **14**, 336 (2018).
[26] N.W. Ashcroft, N.D. Mermin. Solid State Physic. Cengage Learning (2011). 833 p.
[27] Ph.B. Allen. Boltzmann. Boltzmann theory and resistivity in metals. In: Quantum Theory of Real Materials. Kluwer, Boston (1996). P. 219.
[29] C. Jacoboni. Theory of electron transport in semiconductors. Springer series in solid-state sciences. Berlin-Heidelberg, Springer (2010). 588 p.
[29] K. Burke. J. Chem. Phys. **136**, 150901 (2012).
[30] K. Zeeger. Semiconductor Physics: An introduction. Springer (1991). 538 p.
[31] A. Migdal. Sov. Phys. JETP **34**, 996 (1958).
[32] G.M. Eliashberg. Sov. Phys. JETP **11**, 696 (1960).
[33] S. Baroni, S. de Gironcoli, A. Dal Corso. Rev. Mod. Phys. **73**, 515 (2001).
[34] G. Kresse, D. Joubert. Phys. Rev. B **59**, 1758 (1999).
[35] J. Paier, R. Hirschl, M. Marsman, G. Kresse. J. Chem. Phys. **122**, 234102 (2005).
[36] J.P. Perdew, A. Ruzsinszky, G.I. Csonka, O.A. Vydrov, G.E. Scuseria, L.A. Constantin, X. Zhou, K. Burke. Phys. Rev. Lett. **100**, 136406 (2008).
[37] A.M. Rappe, K.M. Rabe, E. Kaxiras, J.D. Joannopoulos. Phys. Rev. B **41**, 1227 (1990).
[38] D. Vanderbilt. Phys. Rev. B **41**, 7892 (1990).
[39] J.P. Perdew, A. Zunger. Phys. Rev. B **23**, 5048 (1981).
[40] B. Himmetoglu, A. Janotti, H. Peelaers, A. Alkauskas, Ch.G. Van de Walle. Phys. Rev. B **90**, 241204 (2014).
[41] R. Cuscó, J. Ibáñez, N. Domenech-Amador, L. Artús, J. Zúñiga-Pérez, V. Muñoz-Sanjosé. J. Appl. Phys. **107**, 063519 (2010).
[42] M. Cococcioni, S. de Gironcoli. Phys. Rev. B **71**, 035105 (2005).
[43] O. Madelung. Landolt–Bornstein Numerical Data and Functional Relationships. Springer, Berlin (1984). V. 17. 666 p.

[44] L. Lindsay, D.S. Parker. Phys. Rev. B **92**, 144301 (2015).
[45] K. van Benthem, C. Elsässer. J. Appl. Phys. **90**, 6156 (2001).
[46] I. Souza, N. Marzari, D. Vanderbilt. Phys. Rev. B **65**, 035109 (1997).
[47] F. Hanzig, J. Hanzig, E. Mehner, C. Richter, J. Vesely, H. Stocker, B. Abendroth, M. Motylenko, V. Klemm, D. Novikov, D.C. Meyera. J. Appl. Crystallography **48**, 393 (2015).
[48] I.-T. Lu, J. Park, J.-J. Zhou, M. Bernardi. Comp. Mater. **6**, 17 (2020).
[49] A.M. Ganose, J. Park, A. Faghaninia, R. Woods-Robinson, K.A. Persson, A. Jain. Nature Commun. **12**, 1 (2021).